1288 *Inorg. Chem.* **2011**, *50*, 1288–1294
DOI: 10.1021/ic101825e

Inorganic Chemistry
Article

Synthesis of Air Stable FeCo/C Alloy Nanoparticles by Decomposing a Mixture of the Corresponding Metal-Acetyl Acetonates under Their Autogenic Pressure

Elena Holodelshikov, Ilana Perelshtein, and Aharon Gedanken*

Department of Chemistry, Kanbar Laboratory for Nanomaterials, Institute of Nanotechnology and Advanced Materials, Bar-Ilan University, Ramat-Gan 52900, Israel

Received September 6, 2010

A mixture of $Fe(AcAc)_2$ and $Co(AcAC)_2$ was thermolyzed in a closed cell under the autogenic pressure of the reactants. The nature of the products was temperature dependent. The reaction is a one-stage, simple, efficient, and solvent-free method to prepare FeCo alloy nanoparticles protected by a carbon shell. Particle sizes of 60−150 were obtained covered by a carbon layer of 3−4 nm. The air stability of these particles is also demonstrated.

Introduction

Metallic nanomaterials have been intensively studied in recent years with respect to their novel properties and potential commercially valuable applications. Metallic alloys are also of importance, because when two or more metals form an alloy, the product might have superior synergetic properties, as compared with the individual metal. To encapsulate these alloys in a protective layer would be beneficial because metals, as well as alloys, might oxidize at ambient conditions. The applications of encapsulated metallic alloy nanoparticles in a protective layer are used in the areas of defense, bioengineering, power electronics, and data storage industries.[1,2] An FeCo alloy is an important soft magnetic material because of its unique magnetic properties, including large permeability and very high saturation magnetization. However, since both iron and cobalt are active metals and oxidize easily in air (nanometric iron is pyrophoric), it is very important to protect them from oxidation. Forming a carbon coating on the surface of these magnetic nanoparticles shields the magnetic nanoparticles against environmental degradation, and keeps the magnetic properties unchanged.

Various methods have been reported in the literature for the formation of core/shell nanostructures. They include sonochemistry,[3,4] electrochemistry,[5] sol−gel methods,[6,7] the carbon-arc method,[8] ammonia catalysis,[9] microwave irradiation,[10] and others. It is worth mentioning that air stable FeCo has already been reported for 15 nm monodisperse particles by the direct formation in solution of crystalline superlattices.[20] Herein, we report on a simple, efficient, solvent-free, and economical synthesis technique for the fabrication of FeCo/C core/shell nanoparticles where the FeCo alloy forms the core. The spherical core/shell structure is obtained in a one-step, solvent-free process when a mixture of two precursors is dissociated at elevated temperatures in a closed cell. The thermolysis reaction was conducted at various temperatures. This reaction is called RAPET (**R**eaction under **A**utogenic **P**ressure at **E**levated **T**emperature). The Fe/Co alloy has been synthesized by various techniques. For example, Kodama et al. used the polyol technique[17] to prepare the alloy having a saturation magnetization of 225 emu/g. The Kratschmer−Huffman carbon arc method[8] was used by McHenry's group. Mechanical alloying[18] and a high temperature reduction[19] were also used in the synthesis of the Fe/Co alloy. Several reports on the formation of core/shell nanostructures of transition metals have already been published.[11,12] For example, the RAPET of cobalt acetate[13] or nickel acetate,[13] nickel acetyl acetonate[16] has led to a Co/C or Ni/C core/shell nanostructure, respectively. Unlike Co and Ni, the pyrolysis of Fe(II)acetate formed Fe_3O_4/C[13] and not Fe/C. The innovation of the current report is the preparation of FeCo/C nanoparticles in the RAPET synthesis. On the basis of the previous results of the decomposition of cobalt acetate[13] and Fe(II)acetate,[13] we expected to

*To whom correspondence should be addressed. E-mail: gedanken@mail.biu.ac.il.

(1) Mchenry, M.; Laughlin, D.; Salazar-Alvarez, G.; Mikhailova, M.; Toprak, M.; Zhang, Y.; Muhammed, M. *Acta. Mater.* **2000**, *48*, 223.
(2) Coey, J. M. D. *J. Magn. Mater.* **2001**, *226*, 2107.
(3) Pol, V. G.; Grisaru, H.; Gedanken, A. *Langmuir* **2005**, *21*, 3635.
(4) Koltypin, Y.; Perkas, N.; Gedanken, A. *J. Mater. Chem.* **2004**, *14*, 2975.
(5) Ting, L. *Trans. Nonferrous Met. Soc. China* **2007**, *17*, 1343.
(6) Zhang, S.; Dong, D.; Sui, Y.; Liu, Z.; Wang, H.; Qian, Z.; Su, W. *J. Alloys Compd.* **2006**, *415*, 257.
(7) Manivannan, S.; Ramaraj, R. *J. Chem. Sci.* **2009**, *121*, 735.
(8) Gallagher, K.; Johnson, F.; Kirkpatrick, E. M.; Scott, J. H.; Majetich, S.; McHenry, M. E. *IEEE Trans. Magn.* **1996**, *32*, 4842.
(9) Wang, P.; Chen, D.; Tang, F. *Langmuir* **2006**, *22*, 4832.
(10) Jacob, D. S.; Genish, I.; Klein, L.; Gedanken, A. *J. Phys. Chem.* **2006**, *110*, 17711.
(11) Pol, S. V.; Pol, V. G.; Gedanken, A. *Chem.—Eur. J.* **2004**, *10*, 4467.
(12) Pol, V. G.; Seisenbaeva, G.; Kessler, V. G.; Gedanken, A. *Chem. Mater.* **2004**, *16*, 1793.
(13) Pol, S. V.; Pol, V. G.; Felner, I.; Gedanken, A. *Eur. J. Inorg. Chem.* **2007**, 2089.

 Published on Web 01/13/2011

obtain an alloyic oxide as the core. Surprisingly, we obtained metallic alloys as the core. Two low-cost acetyl acetonate precursors, $(Fe(AcAc)_2$ and $Co(AcAc)_2$, in different molar ratios, were introduced into a Swagelok reactor union and heated at various temperatures (from 700 to 1000 °C) for 3 h. Different compositions of the metallic core were obtained at the different temperatures.

Experimental Section

The synthesis of the FeCo/C core/shell structure is carried out by the thermal dissociation of a cobalt acetyl acetonate $[Co(AcAc)_2]$ (97%) and iron acetyl acetonate $[Fe(AcAc)_2]$ (99.95%) mixture, using various molar ratios. The acetyl acetonate precursors were purchased from Sigma-Aldrich and used as received. The 1 mL closed vessel cell was assembled from stainless steel Swagelok parts. A 3/8″ union part was plugged from both sides by standard caps. For these syntheses, 0.5 g (total weight) of an acetyl acetonate precursor mixture in various molar ratios (Fe/Co = 1:1; 1:3; 3:1; 1:5; 5:1) was introduced into the cell at room temperature in a nitrogen-filled glovebox. The filled cell was closed tightly by the other plug and then placed inside an iron pipe in the middle of the furnace. The temperature was raised at a heating rate of 10 °C per minute, and the closed cell was heated at 700, 800, 900, and 1000 °C for 3 h. The reaction proceeds under the autogenic pressure of the precursors. The closed vessel cell was gradually cooled (~5 h) to room temperature, and the resulting black powder was collected. Gases were released when opening the cell. All the products were characterized by structural, compositional, morphological, and magnetic measurements without further processing.

X-ray diffraction (XRD) patterns were collected by using a Bruker AXS D* Advance Powder X-ray Diffractometer (Cu Kα radiation, wavelength 1.5406 Å). The morphologies, grain size, and chemical composition were further characterized with a Transmission Electron Microscope (TEM), JEM-1200EX model, and a High-Resolution Transmission Electron Microscope (HRTEM), JEOL 2010 model. The Selected Area Energy Dispersive X-ray Analysis (SAEDS) of an individual particle was conducted using a (HRTEM) JEOL-2010 model. The elemental analysis of the samples was carried out with an Eager 200 analyzer. Magnetization measurements were performed in a Superconducting Quantum Interference Device Magnetometer MPMS-XL.

Results and Discussions

X-ray Diffraction and C, H Analysis. The composite products obtained from the RAPET reactions were characterized by XRD measurements. Figure 1 shows the XRD patterns of the powders prepared at 700 °C for 3 h. The initial molar ratio of the precursors was 1:1, 1:3, 3:1 for $Fe(AcAc)_2/Co(AcAc)_2$, respectively.

The diffraction peaks observed from Figure 1 are assigned to the face-centered cubic Co phase (PDF 89-4307) and face-centered cubic Fe_3O_4 phase (PDF 65-3107).[13] In addition, Figure 1 shows that the intensity of the Co and Fe_3O_4 peaks changes according to the molar ratio of the precursors. In this step, we did not observe any alloyic phase formed between the products.

To investigate the influence of the temperature on the formation of the alloy, we carried out the reaction of a 1:1 molar ratio of the precursors at 800 °C for 3 h (all the other parameters are unchanged). The XRD pattern of this sample is presented in Figure 2. The diffraction peaks that were observed belong to face-centered cubic Fe_3O_4, but we could also identify strong diffraction peaks assigned

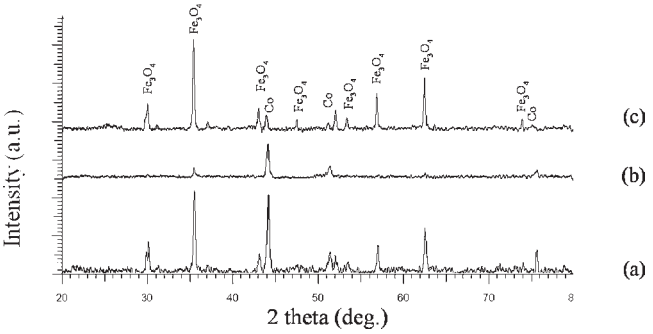

Figure 1. (a) XRD pattern of $Fe(AcAc)_2/Co(AcAc)_2$ (1:1). (b) XRD of $Fe(AcAc)_2/Co(AcAc)_2$ (1:3). (c) XRD pattern of $Fe(AcAc)_2/Co(AcAc)_2$ (3:1) thermolysis. These reactions were done at 700 °C for 3 h.

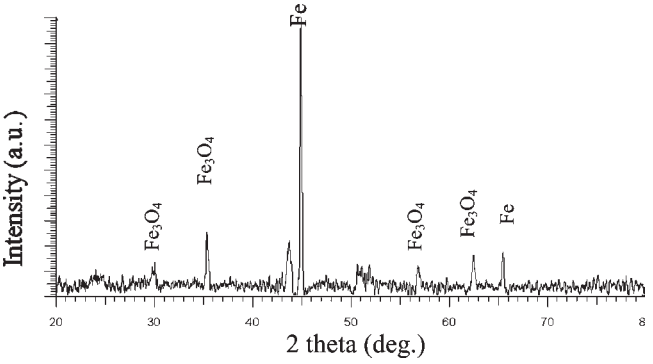

Figure 2. XRD pattern of $Fe(AcAc)_2/Co(AcAc)_2$ (1:1) thermolysis at 800 °C for 3 h.

to the body-centered cubic Fe phase. On the other hand, there was no indication of the presence of Co.

These results led us to conclude that the iron oxide detected at 700 °C was reduced to Fe^0, which formed the FeCo alloy. The disappearance of the Co peaks is attributed to the insertion of Co atoms into the crystal lattice of bcc Fe. However, this pattern can also be attributed to bcc FeCo alloy, since the positions of the XRD peaks are almost identical. In any case whether the product is called an FeCo alloy having the basic structure of bcc Fe perturbed by the Co atoms or bcc FeCo is semantic because both names refer to the existence of an FeCo alloy. To further prove this argument, we have repeated the thermolysis of $Fe(AcAc)_2/Co(AcAc)_2$ (1:1) at 900 °C as well. The XRD pattern of this reaction is presented in Figure 3.

Figure 3 shows the presence of bcc Fe as the only phase, and this is the typical structure of a FeCo alloy. The small diffraction peak at 43−44° shows perhaps the presence of a small amount of carbide Fe_3C (PDF 89-2722). Raising the temperature has caused the complete reduction of iron oxide to Fe (oxidation state 0), and the Co atoms replace the iron atoms in the bcc iron crystal lattice.

We succeeded in minimizing the fabrication of the carbide phase when the reaction of $Fe(AcAc)_2/Co(AcAc)_2$ (1:1) was conducted at 1000 °C for 3 h. The XRD result is presented in Figure 4.

We also measured the XRD of the reaction products conducted for the precursors' molar ratios of 1:5 and 5:1 (Fe/Co) at 1000 °C for 3 h. The XRD patterns for the 5:1 molar ratio showed only the bcc iron, identical to the XRD patterns shown in Figure 3. On the other hand, for

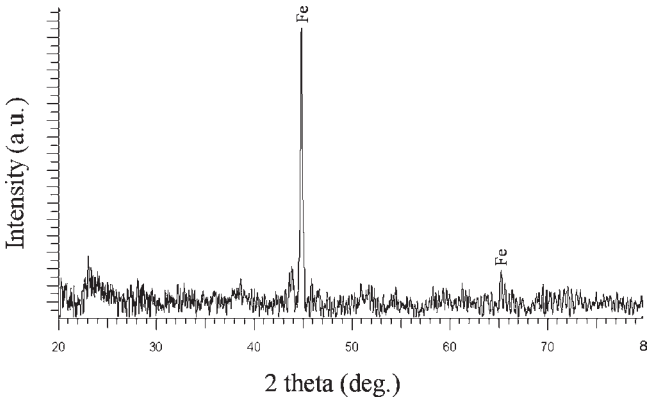

Figure 3. XRD pattern of $Fe(AcAc)_2/Co(AcAc)_2$ (1:1) thermolysis at 900 °C for 3 h.

the 1:5 (Fe/Co) molar ratio, the sole product is fcc of metallic Co.

These results can be explained as follows: when the percentage of Co reaches 80% at 1000 °C, the crystal lattice of Co is observed, and the Fe slightly perturb this crystal structure. The formed alloy acquires the crystal lattice of fcc cobalt, as expected from the phase diagram.[14] Below 80% Co the bcc Fe is detected in the XRD.

From the XRD results we conclude that upon raising the reaction temperature, Fe_3O_4 is reduced to Fe. Once the zerovalent iron is formed it tends to form the FeCo alloy spontaneously. Support for this explanation is obtained from the slight shifts that we detect for the positions of the characteristic XRD peaks of the alloys, in comparison with those observed for the bare metals. These little shifts indicate that upon the insertion of the second atom, small changes in the parameters of the cell's size occur. These small changes are also proof of the formation of the FeCo alloy. In Table 1 we summarize the products obtained for the various starting materials and their ratios, as well as the different temperatures in which these reactions were conducted. The carbon and hydrogen content in the product was determined by elemental analysis measurements. The calculated elemental percentages of carbon in $Fe(C_5H_7O_2)_2$ and $Co(C_5H_7O_2)_2$ are 47.3 and 46.7%, respectively, while the elemental percentages of hydrogen are 5.5 and 5.4%, respectively. The measured percent of carbon in the product obtained from the thermolysis of $Fe(AcAc)_2/Co(AcAc)_2$ (1:1) at 1000 °C is 42.2%, while the percent of hydrogen is 3.7%. Here, the presence of carbon and hydrogen in the product sample is reduced because during the decomposition of the precursor, gases such as C_xH_y (hydrocarbons) and/or H_2, are formed. These gases are liberated upon the opening of the closed vessel cell (Swagelok).

TGA Measurements. The TGA measurements were conducted in a flow of nitrogen. The complete decomposition of the precursors is observed at about 400 °C. The higher weight loss is observed for Fe acetyl acetonate (81%), while a smaller weight loss (71%) is detected for Co acetyl acetonate. The residual weight of about 19% corresponds to the metallic Fe (22% wt. Fe in Fe acetyl acetonate), while the 29% for Co acetyl acetonate is much larger than the Co percentage in Co acetyl acetonate (24% wt.). This larger percentage of the material left after decomposition is attributed to the presence of carbon that is not removed by the nitrogen flow.

TEM, HR-TEM, SAEDS, and Raman Measurements. The morphology of all the samples was studied by TEM measurements.

Figure 5 shows black spheres, or somewhat elongated features, embedded in a more transparent amorphous layer. The black spheres, which have a diameter that ranges from 16 to 52 nm, are the magnetite and cobalt products that are densely embedded in the carbon layer. The agglomeration of the magnetic particles was also observed.

A better separation between the core and the shell is observed for the products of the RAPET reaction conducted at 900 °C. Figure 6 shows that the particles are spherical, and each one of them is surrounded by a layer of about 3−4 nm of disordered carbon. The particle sizes vary from 60 to 150 nm.

Figure 7 illustrates the perfect arrangement of the atomic layers detected in the core. The measured distance between these (110) lattice planes is 0.2028 nm, which is very close to the distance between the planes reported in the literature (0.2027 nm) for the bcc α-Fe lattice (a); a selected area electron diffraction for the FeCo particle is presented (b). The identified planes that correspond to α-Fe are highlighted. In addition, the energy dispersive spectrometry (EDS) analysis of the sample shows the presence of both Fe and Co in each particle. According to the EDS measurement, the Fe/Co ratios in the solid product formed from the 1:1 precursor ratio at 1000 °C are 48 ± 3%:53 ± 3% (% wt), respectively. This result is in good agreement with the initial precursor ratio. Data were collected and averaged over 5 particles. The EDS data prove again that the core is indeed composed of an iron−cobalt alloy, although the XRD shows only the presence of iron.

Figure 8a demonstrates the ordered graphitic layers (3−4 nm thick) around each particle, and which were not observed at lower temperatures. The measured interlayer spacing was 0.34 nm, which is very close to the distance between the graphitic planes reported in the literature (~0.34 nm). It also shows an arrangement of the atomic layers without defects. The EDS analysis of the sample shows again the presence of both Fe and Co in each particle. Figure 8b presents a low resolution TEM image showing a small aggregated ensemble of particles coated with graphitic layers. The particles have a diameter ranging from 15 to 80 nm.

The microscopic measurements support the suggested structure of carbon coated, iron−cobalt alloy formation with temperature elevation. They also show that ordered graphitic layers were formed at a high (1000 °C) temperature.

The nature of the carbon shell is investigated by Raman spectroscopy (Figure 9). The two characteristic bands of carbon were detected at 1340 cm^{-1} (D band), and at 1595 cm^{-1} (G band) for the product of $Fe(AcAc)_2/Co(AcAc)_2$ (1:1) thermolysis at 1000 °C.

The intensity of the D-band associated with disordered carbon is more intense than the G-band associated with graphitic carbon.

(14) Su, X.; Zheng, H.; Yang, Z.; Zhu, Y.; Pan, A. *J. Mater. Sci.* **2003**, *38*, 4581.

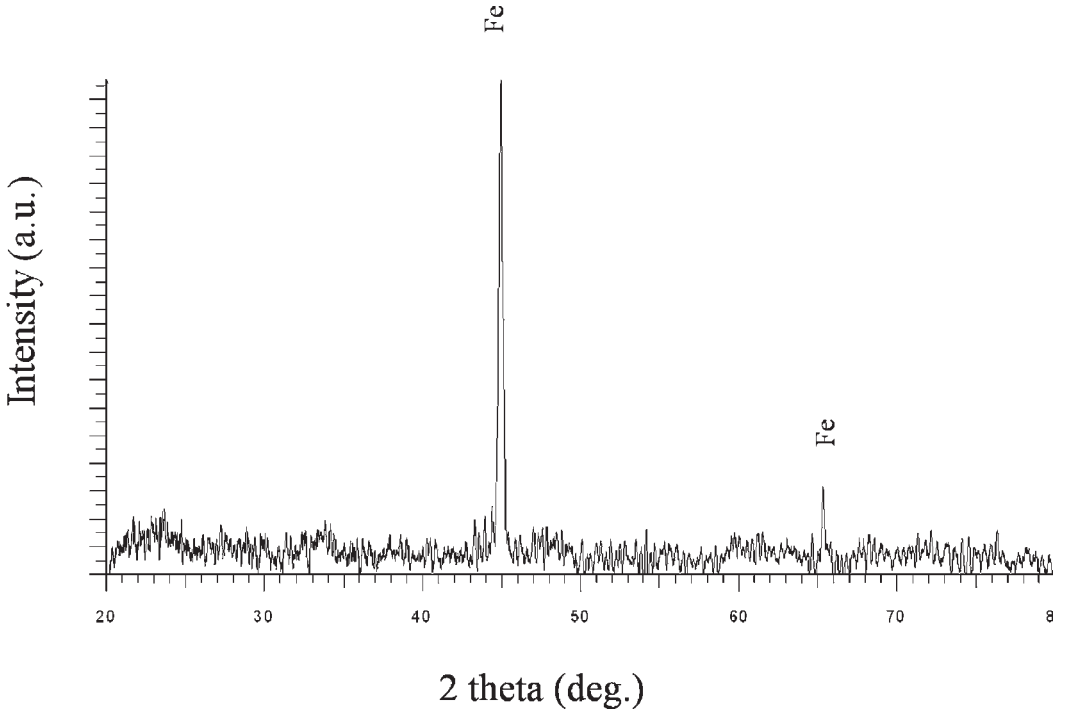

Figure 4. XRD pattern of $Fe(AcAc)_2/Co(AcAc)_2$ (1:1) thermolysis at 1000 °C for 3 h.

Table 1. Summary of the Products of the RAPET Reaction Performed at Various Temperatures and Different Molar Ratios

starting material	temperature of the reaction (in °C)	product obtained from XRD
pure $Fe(acac)_2$	700	Fe_3O_4 (ref 13)
pure $Co(acac)_2$	700	fcc Co
pure $Fe(acac)_2$	1000	bcc Fe
1:1 molar ratio of $Fe(acac)_2$ and $Co(acac)_2$	700	Fe_3O_4+ fcc Co
1:1 molar ratio of $Fe(acac)_2$ and $Co(acac)_2$	900	bcc Fe
$Fe(acac)_2/Co(acac)_2$ = 3:1	700	Fe_3O_4+ fcc Co
$Fe(acac)_2/Co(acac)_2$ = 1:3	700	Fe_3O_4+ fcc Co
$Fe(acac)_2/Co(acac)_2$ = 1:5	1000	fcc Co
$Fe(acac)_2/Co(acac)_2$ = 5:1	1000	bcc Fe

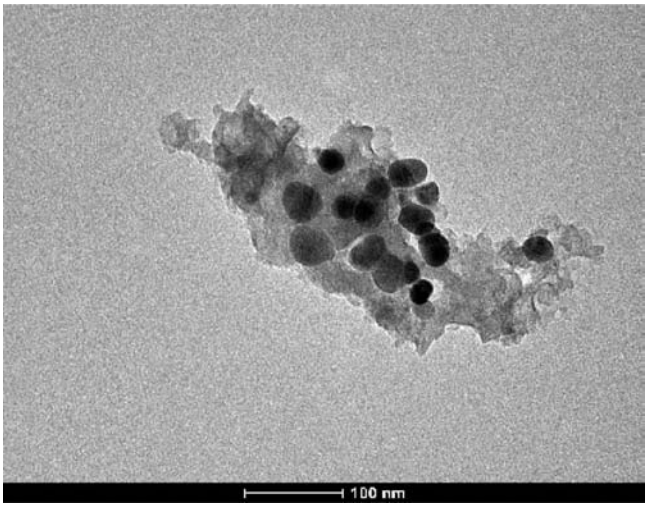

Figure 5. TEM images of $Fe(AcAc)_2/Co(AcAc)_2$ (1:1) thermolysis at 700 °C.

Mössbauer Measurement. The Mössbauer spectrum of $Fe(AcAc)_2/Co(AcAc)_2$ (1:1) thermolysis at 1000 °C is shown in Figure 10. The Mössbauer spectrum was mea-

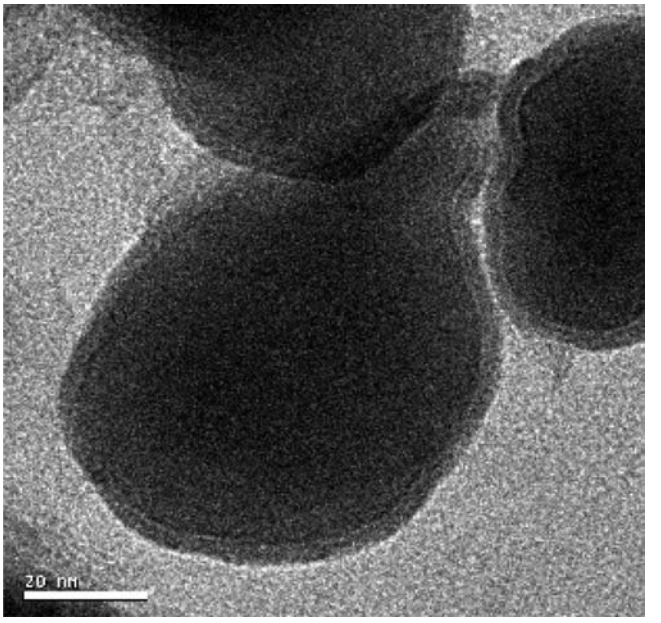

Figure 6. HRTEM image of $Fe(AcAc)_2/Co(AcAc)_2$ (1:1) thermolysis at 900 °C (the scale is 20 nm).

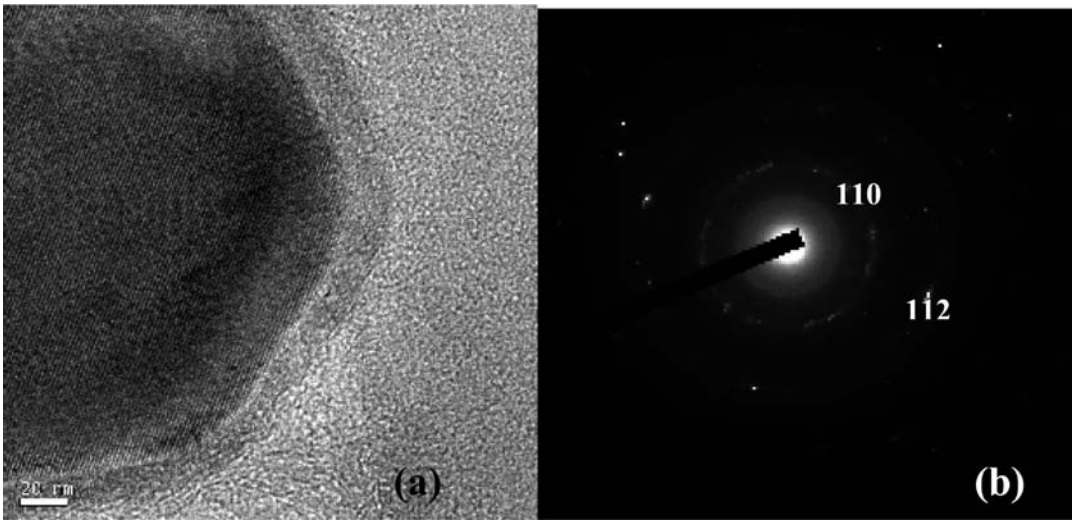

Figure 7. (a) HRTEM; (b) SAED image of $Fe(AcAc)_2/Co(AcAc)_2$ (1:1) thermolysis at 900 °C (the scale is 20 nm).

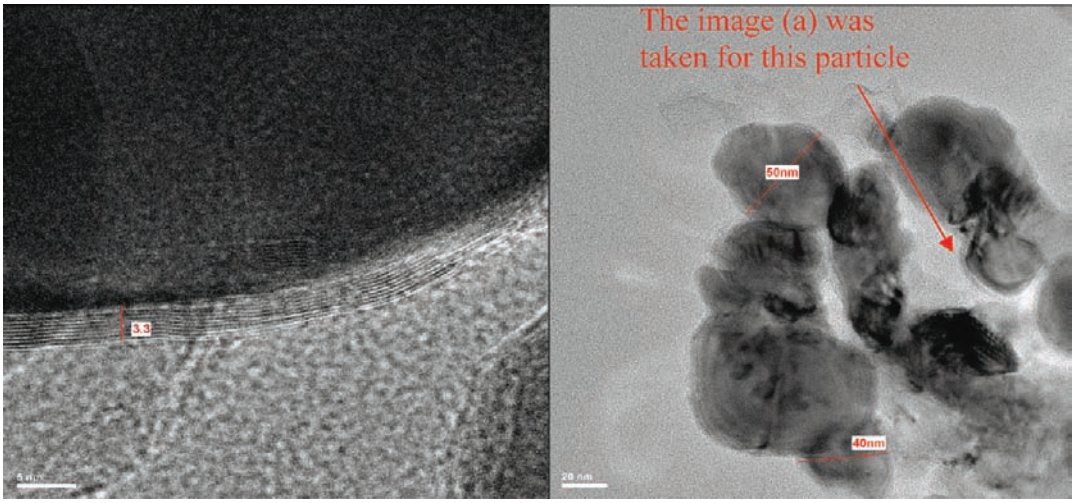

Figure 8. (a) HRTEM (the scale is 5 nm) and (b) low resolution TEM (the scale is 20 nm) images of $Fe(AcAc)_2/Co(AcAc)_2$ (1:1) thermolysis at 1000 °C.

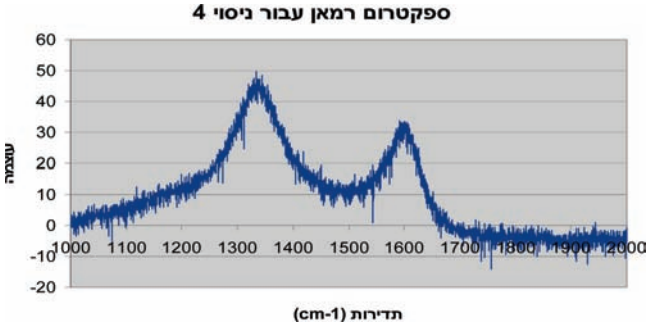

Figure 9. Raman spectra of $Fe(AcAc)_2/Co(AcAc)_2$ (1:1) thermolysis at 1000 °C.

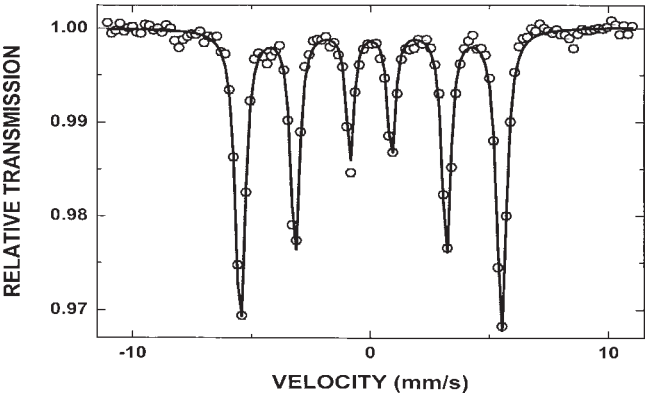

Figure 10. Mössbauer spectrum of $Fe(AcAc)_2/Co(AcAc)_2$ (1:1) thermolysis at 1000 °C at room temperature.

sured at room temperature. Figure 10 demonstrates a magnetic hyperfine field of 330 kOe and no isomer shift; these measurements correspond to pure zerovalent iron (oxidation state 0). The Mössbauer measurements present the additional evidence of FeCo/C formation.

Magnetic Properties. At room temperature, a magnetic susceptibility measurement of a sample prepared at 1000 °C was conducted by employing a Superconducting Quantum Interference Device (SQUID). The magnetization versus magnetic field curve (Figure 11) is measured in the range of −30000 to 30000 Oe.

The sample exhibits typical hysteresis with a saturation magnetization of 115 emu/g (Figure 11). Taking into account the fact that the sample contains 42.2% carbon

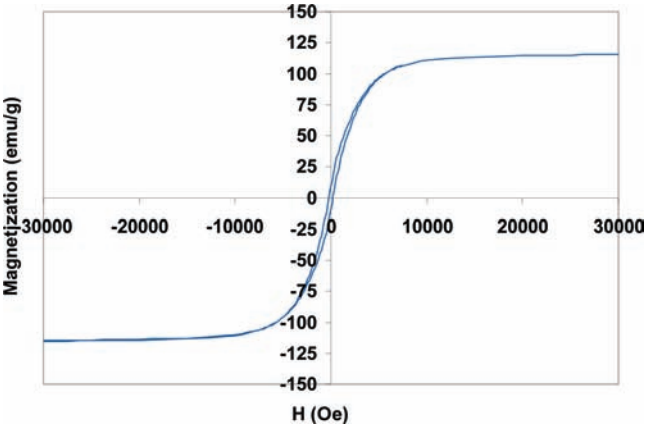

Figure 11. M−H curve for sample $Fe(AcAc)_2/Co(AcAc)_2$ (1:1) prepared at 1000 °C.

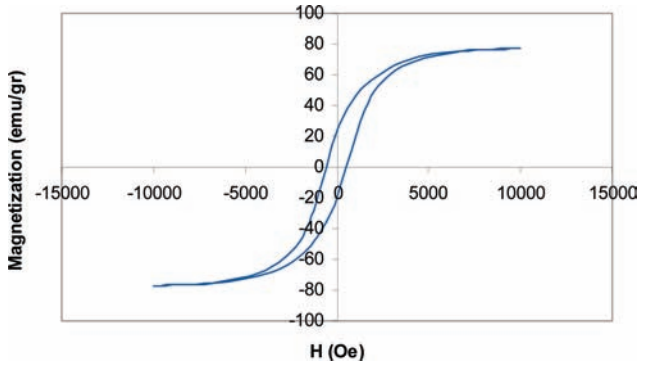

Figure 12. M−H curve for sample $Fe(AcAc)_2/Co(AcAc)_2$ (1:5) prepared at 1000 °C.

and the remaining 57.8% is an iron−cobalt alloy, this yields a value of 199 emu/g for a 100% iron−cobalt particle. This sample shows the coercivity of 170 Oe with a remanent magnetization of 10 emu/g. The particle is large, and therefore typical ferromagnetic behavior, and not superparamagnetic behavior, of the product is detected. The deviation of the saturation magnetization from the bulk value, 225 emu/g, measured by Kodama et al.,[17] may be explained as due to the particle size, or as resulting from an interaction of the ferromagnetic core with the paramagnetic shell. Although it seems that the magnetization curve shifts toward the negative fields, after careful examination no bias is observed.

We also measured the magnetization of a $Fe(AcAc)_2/Co(AcAc)_2$ (1:5) sample prepared by thermolysis at 1000 °C for 3 h. The measurement is presented in Figure 12.

The sample exhibits typical hysteresis with a saturation magnetization of 77 emu/g (Figure 12). When this value is calculated for 100%, 128 emu/g. This magnetization saturation value is much higher than that of bulk Co (65 emu/g), which is its major component. It is clear that this high number is due do the formation of the FeCo alloy, which has a saturation value of (225 emu/g). It can also be explained that the higher value is due to the interaction with the paramagnetic carbon.

A slightly asymmetric hysteresis loop is detected, shifted to the negative magnetic fields. This exchange bias is possibly due to antiferro-ferromagnetic exchange interactions.

Protective Nature of the Carbon Shell. To investigate the protective properties of the carbon (shell) layer we carried out XRD and magnetization measurements for a 1:1 sample (prepared by thermolysis at 1000 °C) 6 months after its preparation. The XRD pattern of the sample aged in open air in the laboratory for 6 months shows diffraction peaks of bcc iron as the only phase (data not shown). No oxide phase was detected after the 6 months. This was not the only measurement conducted to prove the capability of the carbon layer to protect the sample from oxidation, because it might be argued that the oxide formed is amorphous. For this reason we have also performed magnetization measurements for this sample, and the result is presented in Figure 13.

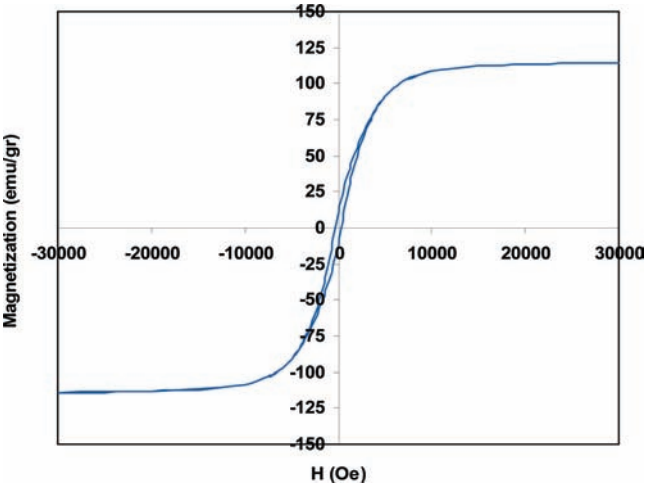

Figure 13. M−H curve for sample $Fe(AcAc)_2/Co(AcAc)_2$ (1:1) prepared at 1000 °C, after 6 months.

Comparing Figures 13 and 11 shows that the saturation magnetization (115 emu/g) and other parameters remained the same after 6 months. We have also examined whether HF can penetrate the FeCo/C by treating it with an aqueous solution of HF (10% vol.). We have not observed any color change of the solution. If Fe^{2+} or Fe^{3+} would have been formed the solution would be either red or blackish red. The stability of the product is undoubtedly proven. The main question arising is why the thermal decomposition[13] of the $Fe(AcAc)_2/Co(AcAc)_2$ mixture at 700 °C leads to Fe_3O_4 formation, while at high temperatures (900−1000 °C) it causes Fe (zerovalent iron) formation.

We propose two possible explanations:

(1) Gases (CO, CO_2) present in the reaction vessel (Swagelok) cause the Boudouard Reaction to occur:

$$2CO \rightleftharpoons CO_2 + C$$

The reaction in the way it is written is exothermic. At high temperatures the endothermic reaction prevails, leading to the formation of carbon monoxide as the dominant product. The CO reduces the iron oxide (Fe_3O_4) to zerovalent iron in the following reaction:

$$Fe_3O_4 + 4CO \rightarrow 3Fe + 4CO_2$$

(2) Carbon is an additional reducing agent at high temperatures[15] as follows:

$$Fe_3O_4 + 2C \rightarrow 3Fe + 2CO_2$$

(15) Stir, M.; Ishzaki, K.; Vaucher, S.; Nicula, R. *J. Appl. Phys.* **2009**, *105*, 124901.

To choose between these two options the following experiment was carried out: the cell with a 1:1 mixture of $Fe(AcAc)_2/Co(AcAc)_2$ was heated to 700 °C for 3 h. The cell was cooled down and then opened to release the residual gases. It was then recapped and the as-synthesized product was heated to 1000 °C for 3 h. The intermediate product was a mixture of Fe_3O_4 and Co (diffraction identical to Figure 1a), while the final product was Fe/C (diffraction identical to Figure 4). The results of this experiment indicate that the carbon is the reducing agent and not the CO that was eliminated upon opening the cell.

A mechanism explaining the creation of the core/carbon shell structures formed in RAPET reactions of various starting materials has already been discussed in several papers.[11] However, we will repeat briefly the idea outlined in these papers: it was proposed that at a high temperature the thermolyzed molecule is atomized. The solidification process is kinetically controlled, and the core is first solidified, followed by the solidification of the shell.

Conclusions

FeCo/C core/shell alloy magnetic nanoparticles are successfully prepared in a one-step process, solvent- and catalyst-free synthesis, by using low cost transition metal acetyl acetonate precursors. The influence of temperature on the alloy's formation was investigated (in the range of 700 to 1000 °C). It was found that iron oxide (obtained at 700 °C) was formed first and was reduced to zerovalent iron by temperature elevation (Boudouard Reaction). Second, Co atoms were inserted into the Fe crystal lattice to form a bcc Fe−Co alloy structure. The reactions presented in the current paper demonstrate the advantages of using the Swagelok union as an autoclave. To the best of our knowledge there is no commercial autoclave that can be used in the temperature range probed in the current research, 700−1000 °C.

(16) Pol, S. V.; Pol, V. G.; Frydman, A.; Churilov, G. N.; Gedanken, A. *J. Phys. Chem. B* **2005**, *109*, 9495.
(17) Kodama, D.; Shinoda, K.; Sato, K.; Sato, Y.; Jeyadevan, B.; Tohji, K. *IEEE Trans. Magn.* **2006**, *42*, 2796.
(18) Li, H. F.; Ramanujan, R. V. *J. Metastable Nanocryst. Mater.* **2005**, *23*, 187.
(19) Bergheul, S.; Haddad, A.; Tafat, H.; Azzaz, M. The 8th International Conference of the Slovenian Society for Non- Destructive Testing, "Application of Contemporary Non-Destructive Testing in Engineering", Portoroz, Slovenia, Sept. 1−3, 2005; p 277.
(20) Desvaux, C.; Amiens, C.; Fejes, P.; Renaud, P.; Respaud, M.; Lecante, P.; Snoeck, E.; Chaudret, B. *Nat. Mater.* **2005**, *4*, 750.